



Supplement of

Wintertime organic and inorganic aerosols in Lanzhou, China: sources, processes, and comparison with the results during summer

Jianzhong Xu et al.

Correspondence to: Jianzhong Xu (jzxu@lzb.ac.cn)

The copyright of individual parts of the supplement might differ from the CC-BY 3.0 licence.

Table S1 Blank and nuclear bomb peak corrected f_{nf} and error (u) obtained from the ^{14}C measurement as well as OC_{nf} (blank corrected) data for all measured filters.

Date	OC ($\mu\text{g cm}^{-2}$)	f_{nf}	u (f_{nf})	OC_{nf} ($\mu\text{g cm}^{-2}$)	u (OC_{nf}) ($\mu\text{g cm}^{-2}$)
1/3/2014	18	0.578	0.020	10.4	1.1
1/8/2014	12	0.507	0.021	6.1	0.7
1/15/2014	10	0.543	0.025	5.4	0.6
1/23/2014	16	0.572	0.020	9.1	1.0

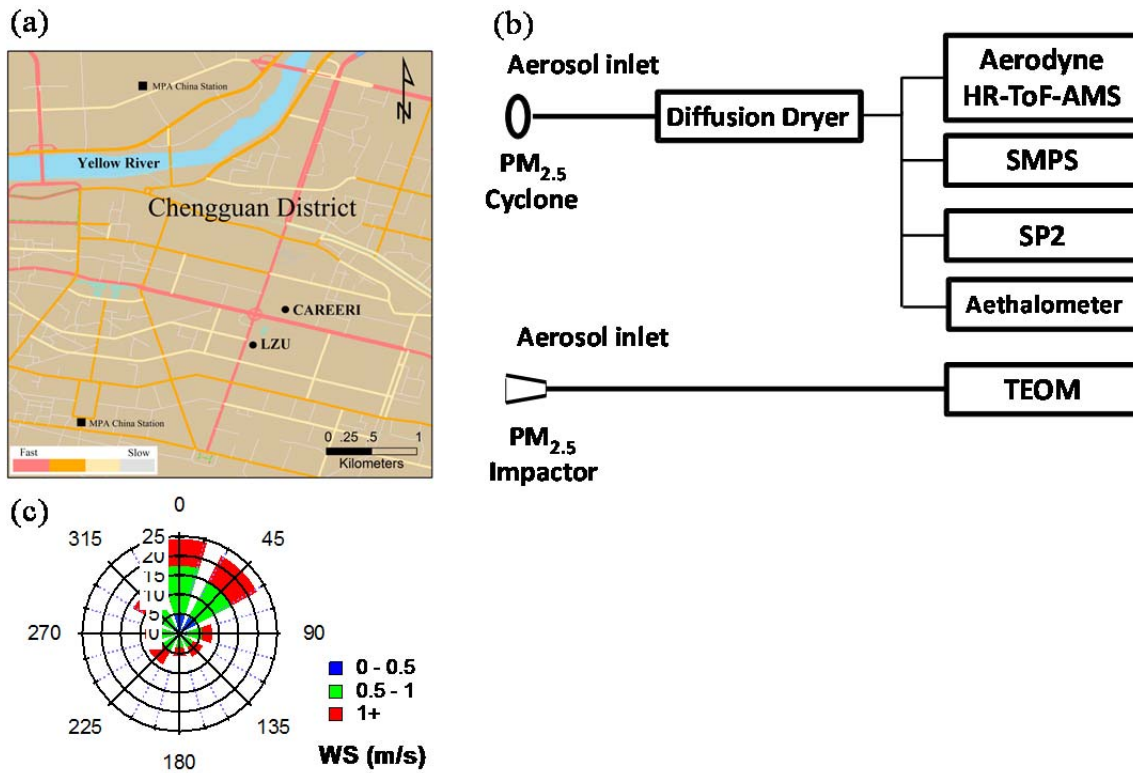


Fig. S1. (a) Location of sampling sites (LZU and CARERI) and MPA China Stations, (b) the setup of instruments, and (c) the wind rose plot during the field study period

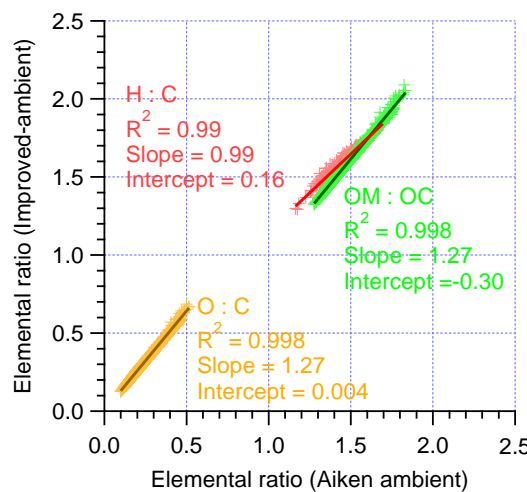


Fig. S2. Scatter plot of values calculated with “Improved-ambient” method versus that with “Aiken ambient” method.

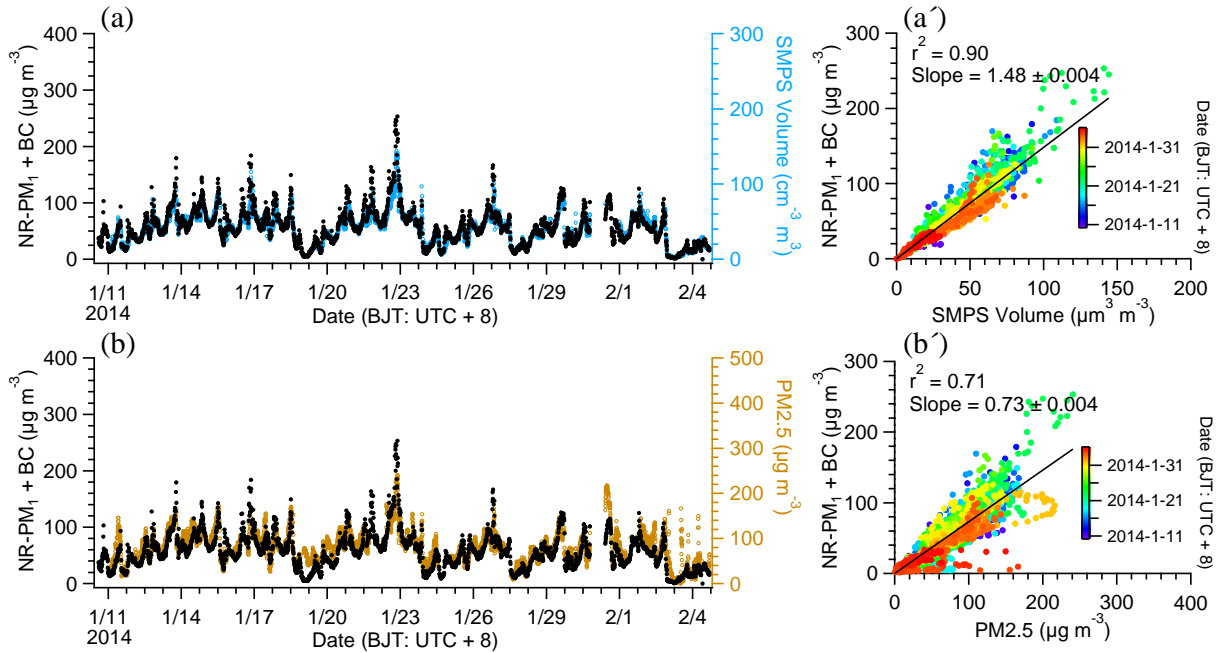


Fig. S3 Inter-comparisons between PM1 (NR-PM1 + BC) mass concentration and the data of acquired by parallel instruments: (a) particle volume by a SMPS and (b) PM2.5 by a TEOM. (a') and (b') are the corresponding scatter plots, respectively.

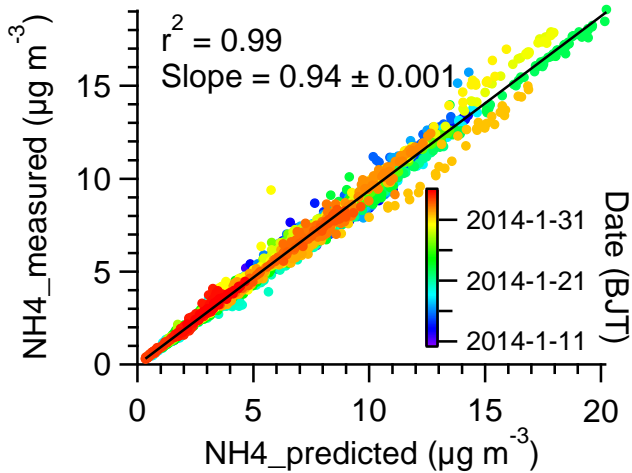


Fig. S4 Scatter plot of measured ammonium versus predicted ammonium using the concentrations of sulfate, nitrate, and chloride. (report RIE in the ms including RIE_NO3, RIE_SO4)

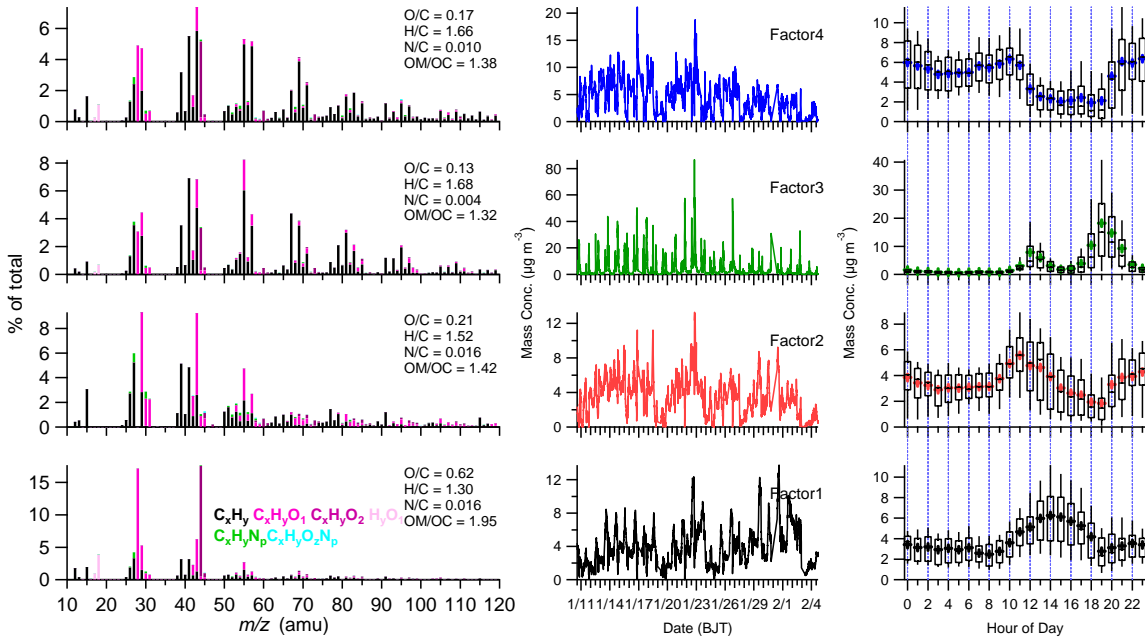


Fig. S5 Four factors solution analyzed by PMF

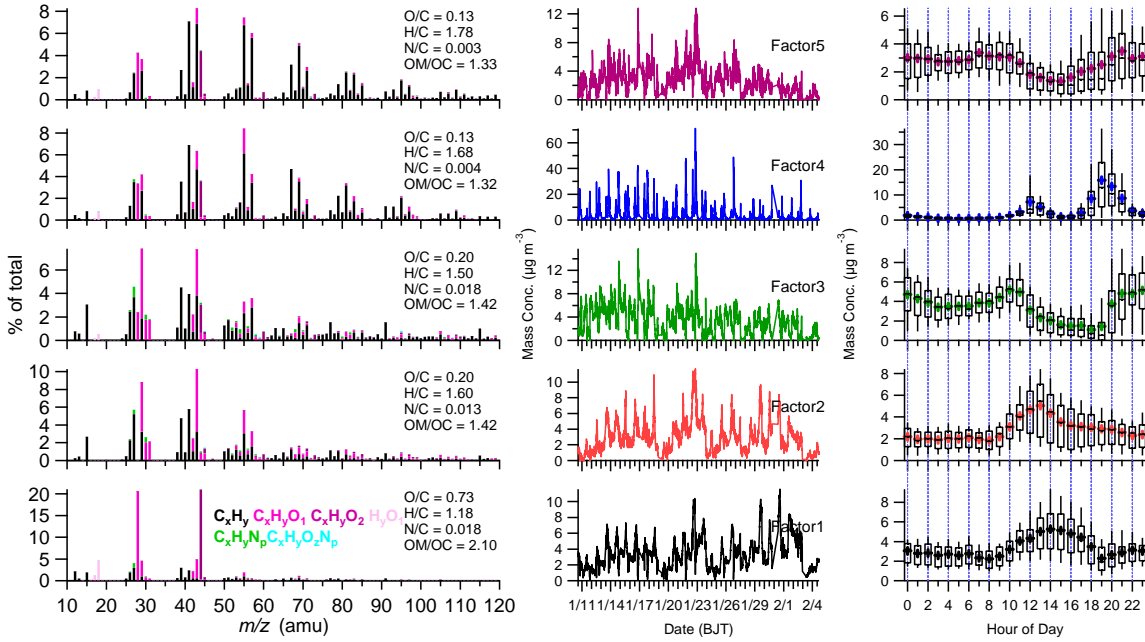


Fig. S6 Five factors solution analyzed by PMF

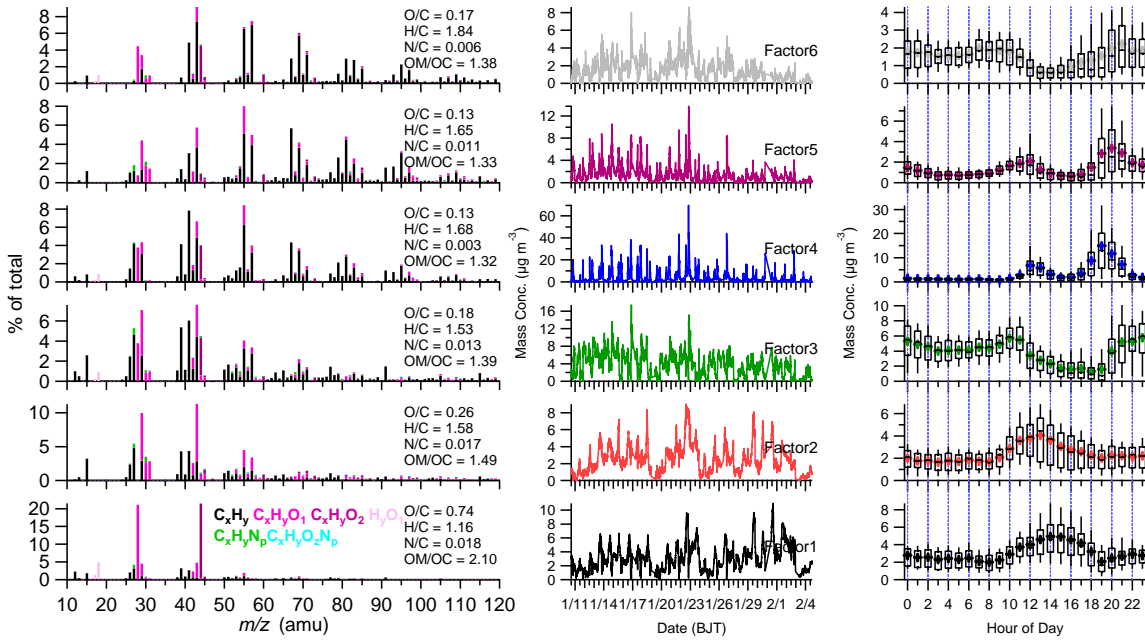


Fig. S7 Six factors solution analyzed by PMF

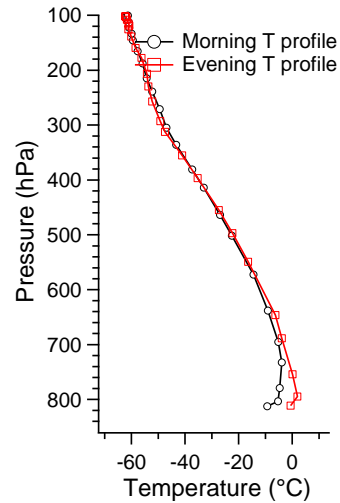


Fig. S8 Averaged air temperature profiles measured at Yuzhong on 8:00 (Morning T profile) and 20:00 (Evening T profile) during January 2014.

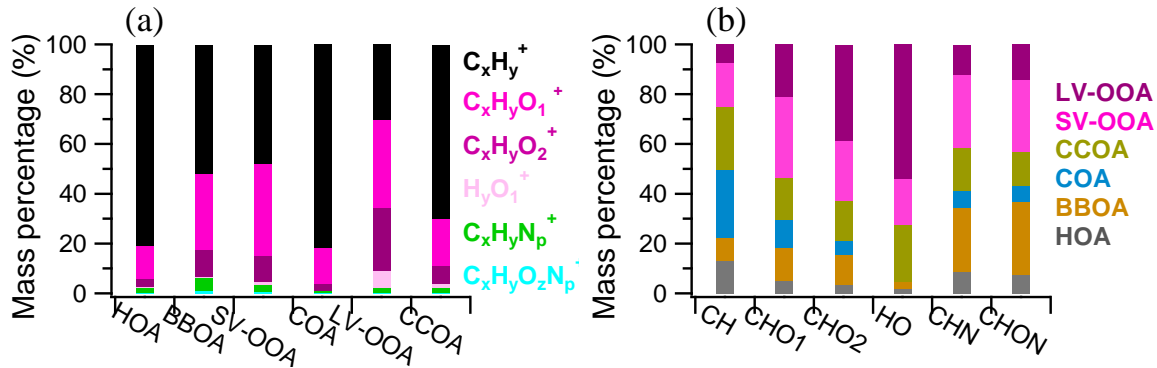


Fig. S9 The contributions of (a) six ionic categories to PMF factors and (b) PMF factors to six ionic categories

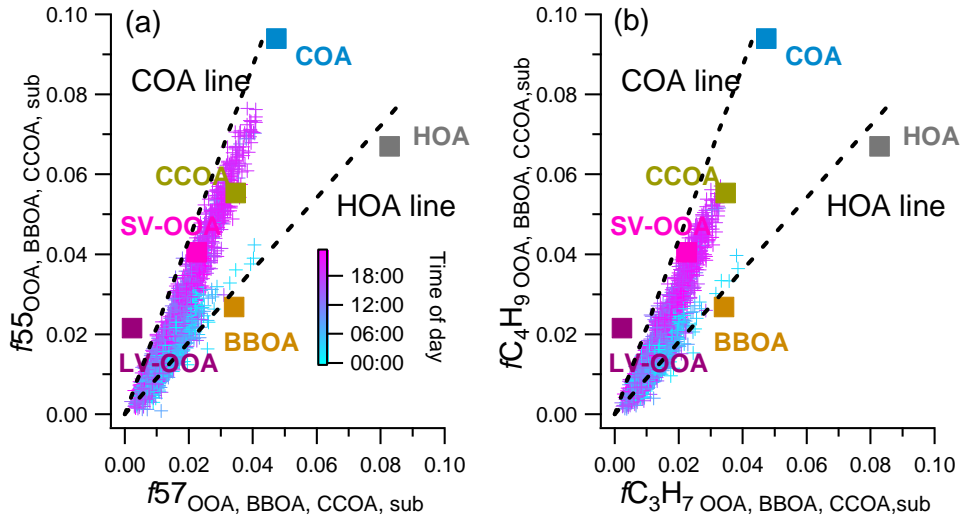


Fig. S10 Scatter plots of (a) $f_{55}^{OOA, BBOA, CCOA, sub}$ vs. $f_{57}^{OOA, BBOA, CCOA, sub}$, and (b) $f_{C_4H_9^{+} OOA, BBOA, CCOA, sub}$ vs. $f_{C_3H_7^{+} OOA, BBOA, CCOA, sub}$. The measured OA data points are colored by time of the day. The corresponding values of the six OA factors identified by PMF in this study are also shown. The HOA and COA lines are adapted from Morh et al., (2012).

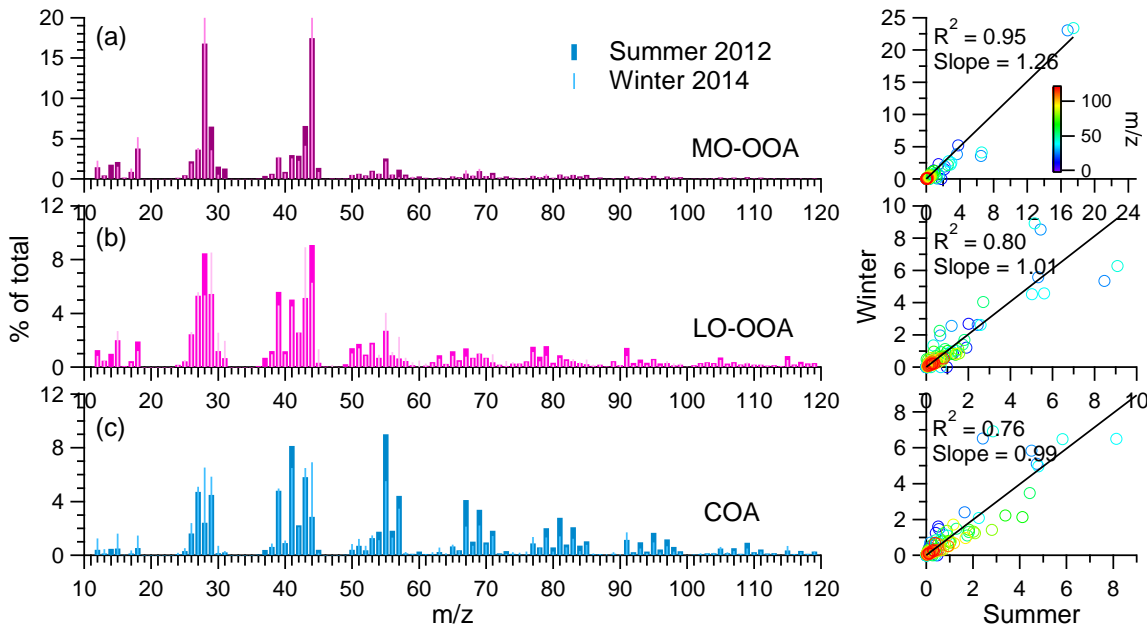


Fig. S11 Comparisons of HR-MS between winter 2013/2014 and summer 2012 for (a) LV-OOA, (b) SV-OOA, and (c) COA.

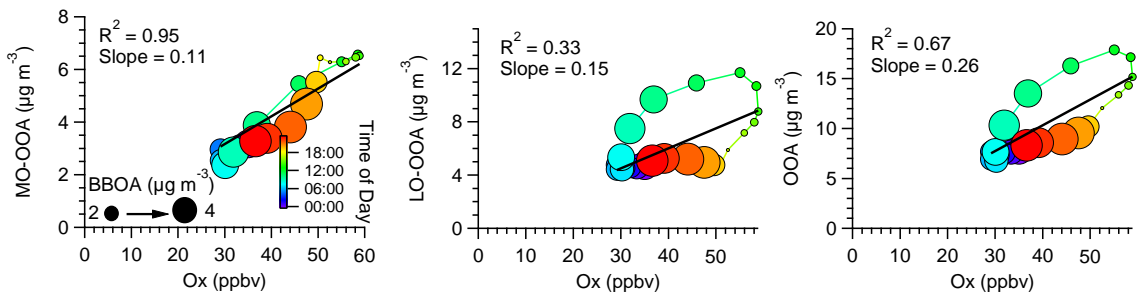


Fig. S12 The correlations between MO-OOA, LO-OOA, and OOA = (LO-OOA + MO-OOA) and Ox.

Reference

Mohr, C., DeCarlo, P. F., Heringa, M. F., Chirico, R., Slowik, J. G., Richter, R., Reche, C., Alastuey, A., Querol, X., Seco, R., Penuelas, J., Jimenez, J. L., Crippa, M., Zimmermann, R., Baltensperger, U., and Prevot, A. S. H.: Identification and Quantification of Organic Aerosol from Cooking and Other Sources in Barcelona Using Aerosol Mass Spectrometer Data, *Atmos Chem Phys*, 12, 1649-1665, 10.5194/acp-12-1649-2012, 2012.